SMiRT-12 / K. Kussmaul (Editor)
1993 Elsevier Science Publishers B.V.

G05/2

EXPERIMENTAL INVESTIGATIONS ON STABLE CRACK GROWTH IN PANELS WITH SEMI-ELLIPTICAL SURFACE CRACKS

K. Wobst, K.-D. Hardtke and P. Wossidlo

Bundesanstalt für Materialforschung und -prüfung (BAM), Berlin, Germany

ABSTRACT

It will be reported about tension tests performed on side-grooved panels made from the German standard steel StE 460 with semi-elliptical surface cracks using the multi specimen methode. These tests resume the analysis about the influence of the triaxiality of the stress state upon the crack resistance and should contribute towards a better understanding and a safer judgement of stable crack growth in structures. In order to represent crack growth investigations on single specimens by a load vs. crack growth curve it was necessary to ensure an adequate geometric reproduction of the initial crack. Thus, it was possible to derive local control curves used as input for the numerical simulation of stable crack growth. The maximum deviation from the initial crack depth $\overline{a}_0$ and from the initial crack width $\overline{c}_0$ resp. came to ±2%. The appearence of a "canoe" shaped crack front under quasi-static load is mainly due to the increase of the constraint caused by the side-grooves of the specimens. On account of the local Δa values determined by the experiments crack mouth opening vs. crack growth curves were derived at several positions Φ along the crack front serving as control curves for the numerical simulation (see paper BG 10/3 of this transactions). For this reason, load vs. crack mouth opening curves were recorded during the tests which show a narrow scatter.

INTRODUCTION

The following investigations belong to a research project within the scope of the analysis and development of fracture mechanics failure concepts supported by the Bundesminister für Forschung und Technologie of the Federal Republic of Germany. They were carried out on the purpose of proceeding with the analysis of the triaxiality of the stress state upon the crack resistance. In order to understand the local as well as the stable crack growth within structures in regard to a safer judgement, a quantitative determination of the influence of the triaxiality on the crack resistance was made in connection with a numerical analysis. Former investigations were carried out by the Fraunhofer-Institut für Werkstoffmechanik, Freiburg and the BAM. The results were obtained by different experimental and numerical analyses on different materials and showed a qualitative relationship between the crack resistance behaviour and the triaxiality of the stress state /1-7/.
Purpose of the experimental investigations:

- Determination of the geometry of a panel with a surface flaw allowing a stable crack to propagate canoe shaped during quasi-static loading when initialized by a fatigue pre-crack.
- Evaluation of the conditions for the processing of a fatigue crack as a test flaw sufficiently equal in geometry into specimens being suitable for the performance of the tests on stable crack growth by the multi specimen procedure.
- Determination of the shape of the stable crack developing within the panel containing a surface flaw as a test failure upon the load conditions.
- Determination of the local crack propagation proceeding perpendicular from the fatigue crack front in dependency on the notch opening.

EXPERIMENTAL RESULTS

The cross-section of the utilized specimen is shown in Fig. 1, its chemical analysis and mechanical properties are given in Table 1. The definition of the cross-section was based upon the capacity of the loading arrangement of 1 MN as well as upon the strength of the material. With regard to a canoe shaped crack propagation the dimensions of the specimen were optimized by the geometry of the surface flaw as well as by the side-grooves lying within the crack plane perpendicular to the vertical center line of the specimen. The starter notches were manufactured by spark erosion using 1 mm resp. 0.1 mm electrodes made from tantalum. While the tension load was active at 22±2°C only poor bending stresses were induced and the following quantities were measured and recorded computer aided: the load F, the notch opening displacements V_1, V_2 and the potential of the DC potential probe at two points lying symmetrically to the middle of the test failure and 2.4 mm away from the surface of the specimen. The use of the potential probe was caused by the need of processing sufficiently equal fatigue cracks as test flaws into several specimens as well as to measure the mean crack growth Δa during quasi-static loading. The calibration of the potential probe was determined during the spark erosive manufacturing of the starter notch into the panel. The velocity of the fixing arrangement of the specimen during the quasi-static loading was 0.0025 mm s^{-1}. Figs. 3 and 4 present the results from tests carried out to determine a specimen appropriate to the purpose of the project. The crack contours were recorded computer aided using a microscope with a magnification factor of 20. As in Fig. 3 no canoe shaped crack growth may be regarded, Fig. 4 shows that side-grooves cause a canoe shape of the stable crack by the induced constraint effect. In Fig. 5 may be seen that it was able to produce fatigue cracks as test flaws of sufficiently equal geometry into 6 specimens. Concerning the depth a_0 (12.15 mm) and the length $2c_0$ (32.5 mm) the deviation was less than 2%. Hence the essential requirement was fulfilled to perform tests on the stable crack growth by the multi specimen methode. The use of the DC potential probe was decisive for the attainment of these results. On condition of a constant DC of I = 120 A the fatigue load acting on the specimens was stopped after ca. 70000 cycles when a specific potential was reached. During the production of the fatigue cracks the maximum load was $F_u = 0.4\ F_{gy}$ (F_{gy}: general yield load) whereas the minimum load was $F_l = 0.04\ F_{gy}$. Fig. 6 shows notch, fatigue crack and stable crack within the side-grooved specimen #1 as well as a scheme and an example for the determination of stable crack growth with respect to the position at the fatigue crack. The canoe shaped crack propagation of the stable crack may well be seen. The notch opening displacements at the surface of the unloaded specimens before and after quasi-static loading were determined using an optical microscope and an electro-mechanical gauge. Fig. 7 shows the results and the positions of the measuring planes for the determination of V_1, V_2 and V_3. It may be recognized that the notch opening displacement was nearly constant along the predominant width. There was no significant difference between the notch opening displacements measured optically resp. electrically. Fig. 8 shows the record of force vs. notch opening displacement ($F\text{-}V_1$) of 5 quasi-statically loaded specimens. It may be seen that the distribution of the curves of all specimens lies within a narrow scatter. The representative curve to the above ones is plotted in Fig. 8b. For the sake of a direct comparison Fig. 9a presents the stable crack growth dependent on the position at the fatigue crack front for two specimens each. Panel #3 and #9 resp. panel #1 and #2 were loaded by almost the same maximum force F_{max} as well as by V_1. The stable crack growth shows no difference between the specimens #3 and #9 on one hand and between the specimens #1 and #2 in a range of $-90° \leq \Phi \leq 0°$ on the other hand. This is no longer valid in case of specimen #1 and #2 in a range of $0° \leq \Phi \leq 90°$. The reason for the distinct difference concerning the crack growth at $\Phi \approx 65°$ was not yet found out. Fig. 9b shows among other things that

- for a relatively small mean value of Δa stable crack growth occurs canoe shaped with its maximum Δa at $\Phi \approx 65°$,
- in case of specimen #1 the Δa of about 6 mm at $\Phi \approx 65°$ is almost three times the value at $\Phi = 0°$.

Figs. 10a and 10b present the stable crack growth vs. notch opening displacement V_1 resp. V_2 which were measured at the same distance from the middle of the test flaw resp. specimen. This figure shows that for equal notch opening displacements Δa increases in dependency on the following order of Φ: 90°, 0°, 45°, 75° and 65°.

SUMMARY

The goals of the experimental investigations were attained:

- A specimen of suitable geometry was determined using a side-grooved panel allowing a surface fatigue flaw to propagate stable and canoe shaped.
- Fatigue cracks of sufficiently equal geometry had to be produced into the specimens as a condition for the realization of the tests on stable crack growth by the multi specimen methode.
- The loading conditions concerning the load as well as the notch opening displacement during the propagation of a stable canoe shaped crack were determined as a representative F-V curve.
- On account of the local Δa values measured during each test crack mouth opening vs. crack growth (V-Δa) curves were derived at several positions Φ along the crack front serving as control curves for the numerical simulation.

The results of the numerical analysis of the crack growth in the experimentally investigated side-grooved tension panel with a surface flaw is presented on this conference by Mr. Moussavi /8/.

REFERENCES

/1/ Kordisch, H.; Sommer, E.; Schmitt, W. (1987): Einfluß der Mehrachsigkeit auf das stabile Rißwachstum. 13. MPA-Seminar, MPA Stuttgart (Germany), pp. 7.1-7.17.

/2/ Brocks, W.; Künecke, G.; Noack, H.-D.; Veith, H. (1987): Zur Übertragbarkeit von Bruchmechanikparametern von Proben auf Bauteile aufgrund von FEM-Analysen. 13. MPA-Seminar, MPA Stuttgart (Germany), pp. 3.1-3.24.

/3/ Memhard, D.; Klemm, W. (1989): Numerische und experimentelle Untersuchungen zum Verhalten von Oberflächenrissen in Zugscheiben und Rohren aus ferritischen und austenitischen Stählen. Freiburg (Germany), Fraunhofer-Institut für Werkstoffmechanik, Bericht W 4/89.

/4/ Brocks, W.; Künecke, G.; Wobst, K. (1989): Stable crack growth of axial surface flaws in pressure vessels. Int. J. Pres. Ves. and Piping 40, pp. 77-90.

/5/ Aurich, D. et. al. (1990): Analyse und Weiterentwicklung bruchmechanischer Versagenskonzepte. Berlin (Germany), Bundesanstalt für Materialforschung und -prüfung, BAM-Forschungsbericht 174.

/6/ Schmitt, W.; Brocks, W. (1991): Analyse und Weiterentwicklung bruchmechanischer Versagenskonzepte, Schwerpunkt: Anwendung des J-Integral-Konzeptes und seine Erweiterungen auf bauteilrelevante Situationen. Freiburg (Germany), Fraunhofer-Institut für Werkstoffmechanik, Bericht W 7/89.

/7/ Brocks, W.; Krafka, H.; Künecke, G.; Wobst, K. (1992): Stable crack growth of axial flaws in pressure vessels. Nucl. Engrg. Des. 135, pp. 151-160.

/8/ Moussavi Zadeh, G. (1993): Analysis of stable crack growth of a semi-elliptical surface crack by numerical simulation. SMIRT12, paper BG 10/3.

Table 1: German standard steel StE 460 - chemical composition (mass%) and mechanical properties [T-direction, (20±2)°C, $\dot{\varepsilon} = 2x10^{-4}\ s^{-1}$]

C	Mn	Ni	Si	V	Cr	Cu	Al	P	S
0.17	1.52	0.62	0.28	0.18	0.04	0.03	0.01	0.009	0.009

Lower yield point	R_{eL}	,	MPa	470±10
Ultimate tensile strength	R_m	,	MPa	635±12
Elongation	A_{10}	,	%	21±2
Lüders strain	$\varepsilon_{Lü}$	,	%	1.9±0.2
Reduction of area	Z	,	%	67±3

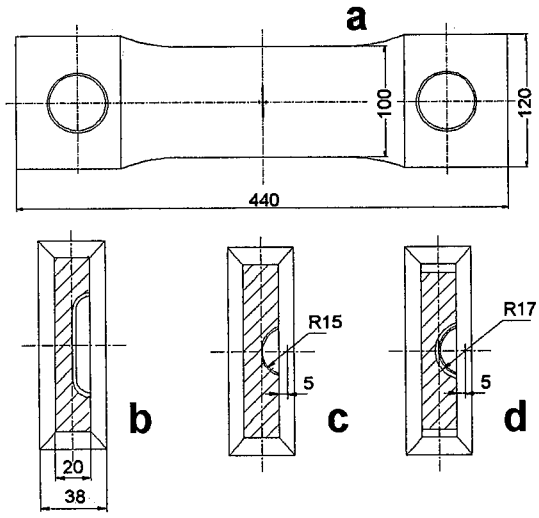

Fig. 1. Principal dimensions of the panel including a surface failure (a); b: specimen without side-grooves; c, d: side-grooved specimen before and after fatigue precracking, resp.

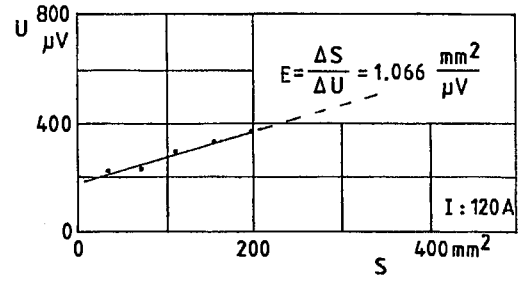

Fig. 2. Calibration of the DC potential probe during machining of the initial notch by spark erosion

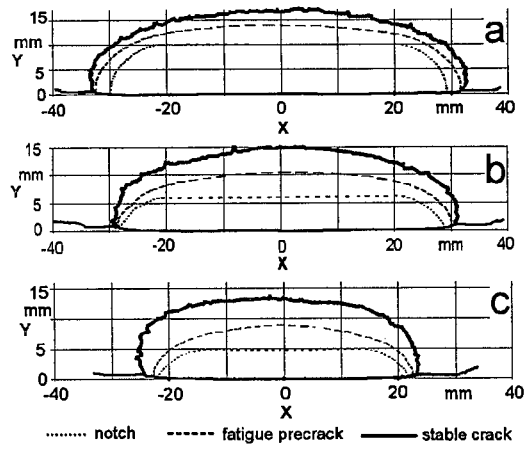

Fig. 3	a_0 mm	$2c_0$ mm	a_0/c_0	a_0/B_0
a	14.22	63.5	0.45	0.71
b	10.57	58.4	0.36	0.52
c	9.05	45.4	0.38	0.45

Fig. 3. Contours of notches, fatigue cracks, and stable cracks within non side-grooved tension panels of different test flaws

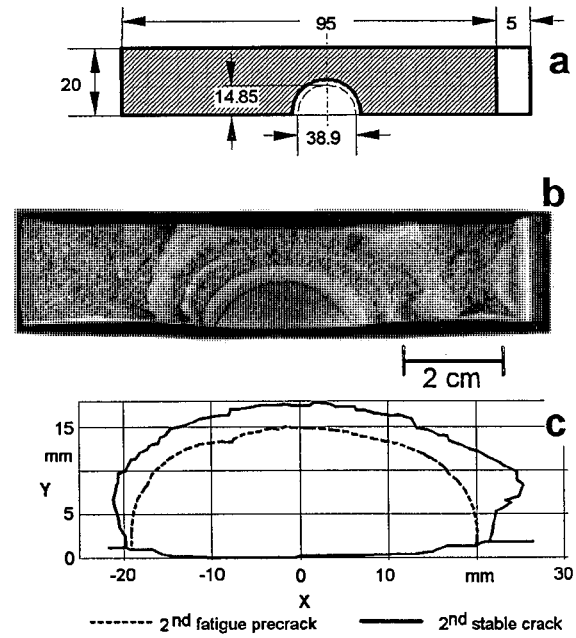

Fig. 4. Cross-section of the specimen (a) as well as view (b) and contours (c) of the fatigue cracks respectively stable cracks (F_{max} 880kN, V_{1max} 1.52mm)

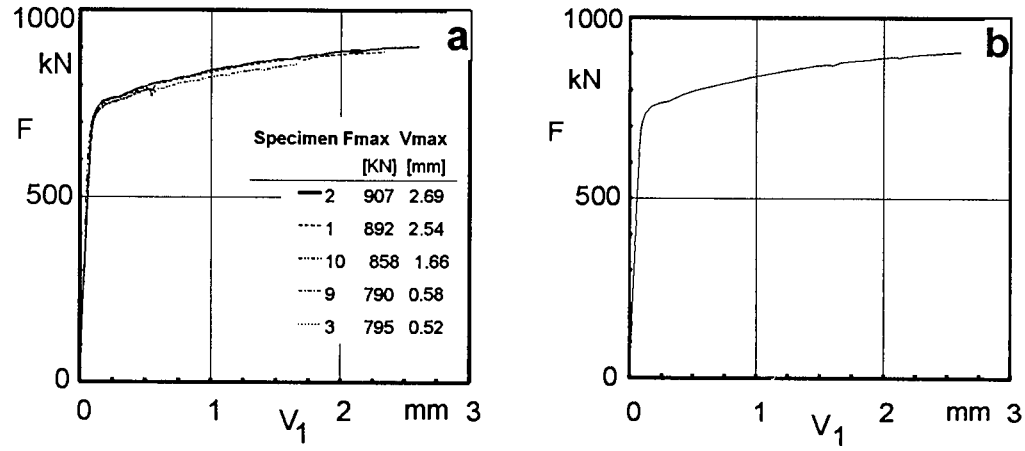

Fig. 8. Record of load vs. notch opening displacement of quasistaticly loaded with surface cracks; a: separate results of 5 specimens; b: representative curve

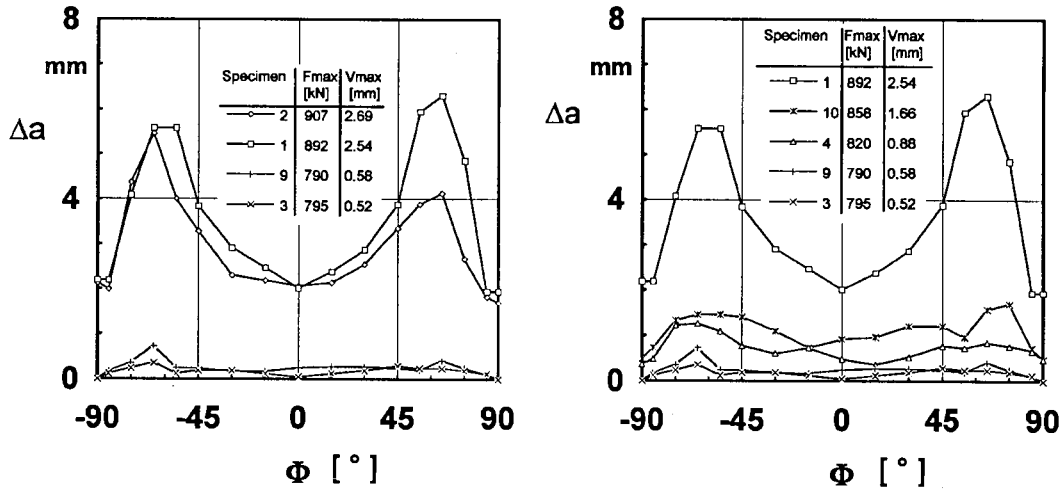

Fig. 9. Stable crack growth Δa in tension panels with surface flaws up to maximum load; dependency on the circumferential position Φ at the fatigue crack

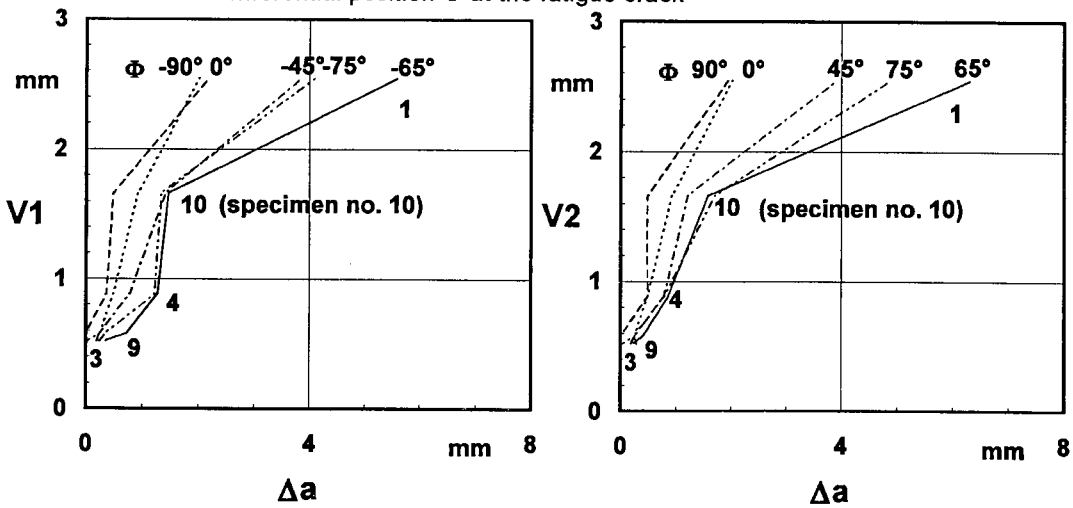

Fig. 10. Notch opening displacement vs. crack growth (V-Δa) curves of different circumferential positions Φ at the fatigue crack

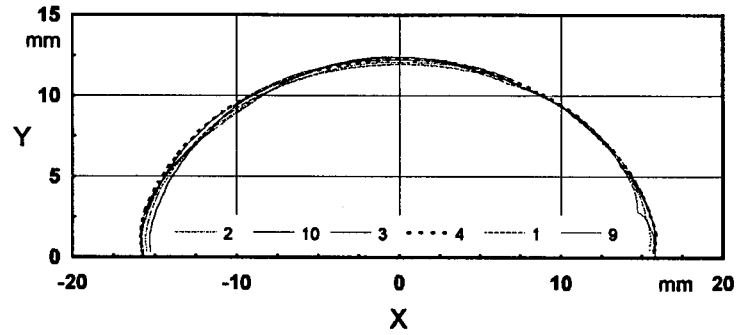

Fig. 5. Contours of the fatigue cracks (test flaws) of 6 panels (1-4, 9, 10) as a function of the distance from the notch center x

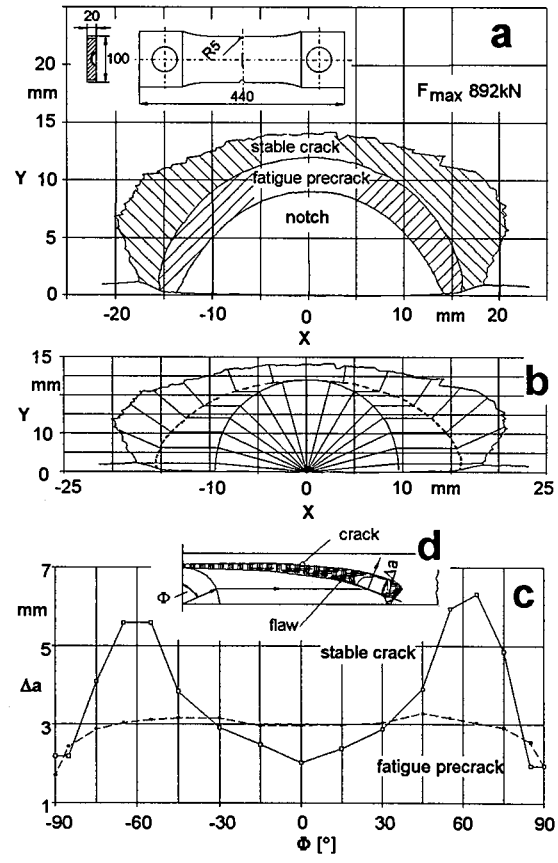

Fig. 6: Fatigue crack and stable crack within panel # 1 (a); illustration for the evaluation of crack growth in dependency on the position at the fatigue crack Φ (b, c)

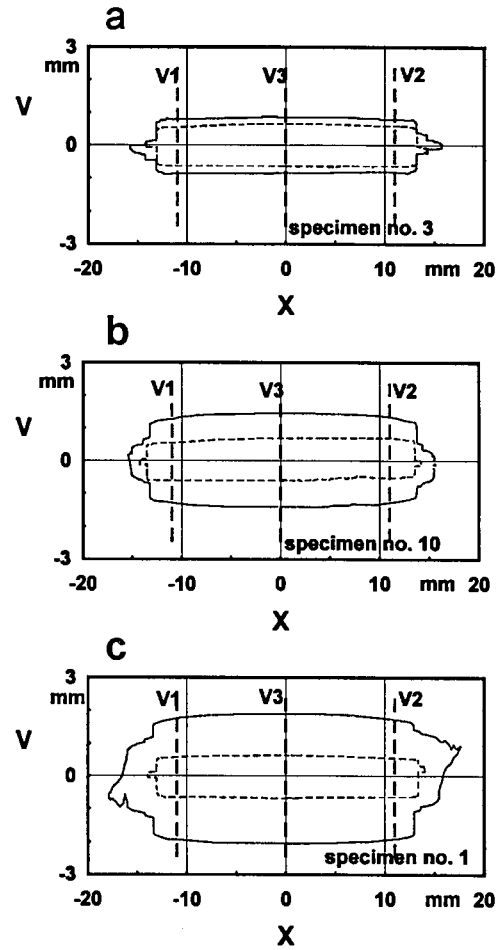

specimen	V1elektr. mm	V1optic. mm	V3optic. mm
1	2.38	2.45	2.62
10	1.54	1.41	1.56
3	0.48	0.48	0.41

Fig. 7. Notch opening displacement at the surface of the unloaded specimens before (---) resp. after (——) a quasi-static tension load as well as the positions of the gauge planes for the determination of V_1, V_2 and V_3